Minimizing Voltage Loss in Efficient All-inorganic $CsPbI_2Br$ Perovskite Solar Cells through Energy Level Alignment

Wenzhan Xu[1,2], Fang He[1,2], Meng Zhang[1,2], Pengbo Nie[1,2], Siwei Zhang[1,2], Cong Zhao[1,2], Ripeng Luo[1,2], Jingzhou Li[1,2], Xuan Zhang[1,2], Shichao Zhao[3], Wen-Di Li[4], Feiyu Kang[1,2,5], Ce-Wen Nan[5], Guodan Wei[1,2*]

[1] Tsinghua-Berkeley Shenzhen Institute (TBSI), Tsinghua University, Shenzhen, 518055, P. R. China
[2] Tsinghua Shenzhen International Graduate School, Tsinghua University, Shenzhen, 518055, P. R. China
[3] College of Materials & Environmental Engineering, Hangzhou Dianzi University, Hangzhou, 310018, P. R. China
[4] Department of Mechanical Engineering, The University of Hong Kong, Pokfulam, Hong Kong, China
[5] School of Materials Science and Engineering, Tsinghua University, Beijing 100084, China

e-mail: weiguodan@sz.tsinghua.edu.cn

Methods

Materials. Lead iodide (PbI_2, 99.999%) and tin (IV) oxide (SnO_2) colloid precursor were purchased from Alfa Aesar; Cesium iodide (CsI, 99.999%), Cesium bromide (CsBr, 99.999%), chlorobenzene (CB, 99.8%), anhydrous dimethyl sulfoxide (DMSO, ≥ 99.9%), *N, N*-dimethylformamide (DMF, 99.8%), 4-tert-butylpyridine (tBP), tris(2-(1H-pyrazol-1-yl)-4-tert-butylpyridine)cobalt(iii)-tris(bis(trifluoromethylsulfonyl) imide) (FK209) and bis(trifluoromethylsulfonyl)amine lithium salt (Li-TFSI) were purchased from Sigma Aldrich. Anhydrous methanol, ethanol (>99.5%) and isopropyl alcohol (IPA, 99.5%) were purchased from Acros; Spiro-MeOTAD (99.8%) was purchased from Xi'an Polymer Light Technology Corp. All materials and reagents were used as received without further purification.

Perovskite precursor preparation. x M (x=0.95, 1, 1.05, 1.1) PbI_2 and 1 M CsBr were dissolved in a mixture of DMF and DMSO (1:9 v/v), followed by magnetically stirred at 70 °C for ~ 12 hours (hrs) till the cloudy solution yields to transparent yellow solution. CsI was dissolved in mixed solvent (methanol:ethanol=1:4 by volume) with a concentration of 1, 2, 3 and 5 mg mL^{-1}.

Fabrication of perovskite solar cells. 40 nm SnO_2 layer is spin-coated onto pre-cleaned and UV-Ozone treated ITO-coated glass substrates from SnO_2 colloid solution with the concentration of 2 mg mL^{-1} at 3000 RPM for 30 seconds (s), followed with thermal annealing at 150 °C for 30 minutes (min) on the hotplate in ambient atmosphere. After the SnO_2/ITO substrate transformed into the N_2 glovebox, $CsPbI_2Br$ is spin-coated on the top of the which at spin-speed of 1500 RPM for 15 s and 5000 RPM for 45 s continuously, followed with thermal annealing firstly at low temperature of 50 ℃ till the color of the thin film transformed into light brown and second high temperature of 260 ℃ for 5 mins on the hotplate. For the target PSCs fabricated with $CsPbI_2Br/CsPbI_3$ thin film, CsI was spin-coated on the top of $CsPbI_2Br$ thin film, followed at 300 °C annealing treatment for 3 min. It was worthy noticed that IPA was dropped onto the as-cast perovskite precursor film with last 20 s finishing the spinning-perovskite films. For deposition of hole-transporting material, Spiro-MeOTAD was dissolved in chlorobenzene with a concentration of 80 mg/mL, then 35 μL of lithiumbis (trifluoromethanesulfonyl) imide in acetonitrile (260 mg/mL) and 30 μL of 4-tert-butylpyridine was added into the Spiro-MeOTAD

solution. The mixture was coated onto the perovskite film at 3500 RPM for 30 s to form a Spiro-MeOTAD hole-transporting layer. Finally, the counter electrode was deposited by thermal evaporation of 80-nm-thick gold under a pressure of $2x10^{-6}$ mbar. The active area was measured to be 0.045 cm^2.

Characterization of perovskite thin films. UV-vis absorption and photoluminescence (PL) spectra of thin films were recorded on a HP 8453 spectrophotometer and FLS920 spectrofluorimeter (Edinburgh Instruments), respectively. A 150 W, ozone-free xenon arc lamp was used in PL measurements. Scanning electron microscope (SEM) images were obtained by using a field emission scanning electron microscope (JEOL-7401). Thicknesses of thin films were measured by Dektak 150 surface profilometer. The X-ray photoelectron spectroscopy (XPS) measurements are performed on an ESCALAB MK II (VG Co., Ltd, England) spectrometer, with Al Ka excitation radiation under ultrahigh vacuum condition. UPS measurements were performed in a high vacuum chamber with a He(I) (21.21 eV) discharge lamp and have a resolution of 0.1 eV. A −10 V bias was applied to the sample to enable accurate determination of the low-kinetic-energy photoelectron cut-off.

Characterization of perovskite solar cells. The *J-V* characteristics of PSCs were measured by a Keithley model 2400 source measure unit (Newport, Oriel AM 1.5G, 100 mW/cm^2). The light intensity of 100 $mWcm^{-2}$ was calibrated by a silicon reference cell. The external quantum efficiency (EQE) is obtained by using EQE measurement system. The cells were connected to a digital oscilloscope (Tektronix TDS 3052C) and the input impedance of the oscilloscope was set to 1 MΩ and 50 Ω, respectively, for monitoring the charge density decay and charge extraction time. The transient photovoltage was measured under 0.3 sun background illumination. An attenuated laser pulse (500 nm) was used as a small perturbation to the background illumination on the device. The laser-pulse-induced photovoltage variation (DV) was smaller than 5% of the V_{OC} produced by the background illumination. The transient photocurrent was measured by applying 500 nm laser pulses with a pulse width of 120 fs and a low pulse energy to short circuit devices in the dark. The laser pulses were generated from an optical parametric amplifier (TOPAS-Prime) pumped by amode-locked Ti:sapphire oscillator seeded regenerative amplifier with a pulse energy of 1.3 mJ at 800 nm and a repetition rate of 1 kHz (Spectra Physics Spitfire Ace).

Table s1. A summary of the detail performance parameters of reported $CsPbI_2Br$ PSCs

Device structure	Bandgap (eV)	Voltage (V)	E_{loss} (V)	Efficiency (%)	Refs
ITO/PEDOT:PSS/$CsPbI_2Br$/PCBM/BCP/Ag	1.90	**1.06**	**0.84**	6.8	1
FTO/c-TiO_2/$CsPbI_2Br$/Spiro-MeOTAD/Ag	1.92	**1.11**	**0.81**	9.84	2
FTO/c-TiO_2/$CsPbI_2Br$/Spiro-MeOTAD/Ag	1.90	**1.10**	**0.80**	10.34	3
FTO/c-TiO_2/$CsPbI_2Br$/Spiro-MeOTAD/Au	1.92	**1.23**	**0.69**	10.7	4
FTO/c-TiO_2/$CsPbI_2Br$/Spiro-MeOTAD/Au	1.92	**1.19**	**0.73**	10.3	5
FTO/c-TiO_2/$CsPbI_2Br$/P3HT/Au	1.90	**1.01**	**0.89**	7.7	6
FTO/c-TiO_2/$CsPbI_2Br$/Spiro-MeOTAD/Ag	1.90	**1.13**	**0.77**	10.5	7
ITO/c-TiO_2/$CsPbI_2Br$/Spiro-MeOTAD/Au	1.92	**1.05**	**0.87**	9.08	8
FTO/NiO_x/$CsPbI_2Br$/ZnO@C_{60}/Ag	1.92	**1.14**	**0.78**	13.3	9
FTO/NiMgLiO/$CsPbI_2Br$/PCBM/BCP/Ag	1.90	**0.98**	**0.92**	9.14	10
ITO/SnO_2/$CsPbI_2Br$/Spiro-MeOTAD/Au	1.90	**1.10**	**0.80**	10.99	11
ITO/SnO_2/$CsPbI_2Br$/Spiro-MeOTAD/Au	1.92	**1.22**	**0.70**	14.21	12
FTO/SnO_2/$CsPbI_2Br$/Spiro-MeOTAD/Ag	1.91	**1.29**	**0.62**	12.34	13
ITO/NiO_x/$CsPbI_2Br$/C_{60}/BCP/Ag	1.90	**1.05**	**0.85**	10.4	14
ITO/SnO_2/ZnO/$CsPbI_2Br$/Spiro-MeOTAD/MoO_3/Ag	1.92	**1.23**	**0.69**	14.6	15
FTO/c-TiO_2/$CsPbI_2Br$/Carbon	1.91	**1.15**	**0.76**	10	16
FTO/c-TiO_2/m-TiO_2/$CsPbI_2Br$/Spiro-MeOTAD/Au	1.91	**1.24**	**0.67**	12.52	17
FTO/c-TiO_2/$CsPbI_2Br$/$CsPbI_3$ QDs/PTAA/Au	1.91	**1.20**	**0.71**	14.45	18
FTO/c-TiO_2/$CsPbI_2Br$/$CsPbX_3$/PTAA/Au	1.91	**1.22**	**0.69**	14.81	19
FTO/c-TiO2/$CsPbI_2Br$/Spiro-MeOTAD/Ag	1.91	**1.07**	**0.84**	12.6	20
ITO/c-TiO_2/$CsPbI_2Br$/Spiro-MeOTAD/Au	1.92	**1.23**	**0.69**	16.07	21
FTO/NiO_x/ln-$CsPbI_2Br$/ZnO@C_{60}/Ag	1.92	**1.15**	**0.77**	13.57	22
FTO/SnO_2/$CsPbI_2Br$/P3HT/Spiro-MeOTAD/Au	1.90	**1.02**	**0.88**	5.3	23
FTO/c-TiO_2/m-TiO_2/$CsPbI_2Br$/P3HT/Au	1.90	**0.96**	**1.083**	7.7	24
FTO/c-TiO_2/$CsPbI_2Br$/$CsPbI_2Br$ QDs/PTAA/Au	1.91	**1.11**	**0.80**	11.88	25
FTO/c-TiO_2/m-TiO_2/$CsPbI_2Br$/HTM/Au	1.91	**1.17**	**0.74**	12	26
ITO/c-TiO_2/$CsPbI_2Br$/Spiro-MeOTAD/Au	1.91	**1.19**	**0.72**	12.39	27
FTO/c-TiO_2/$CsPbI_2Br$/Spiro-MeOTAD/Au	1.91	**1.21**	**0.70**	9.5	28
ITO/SnO_2/$CsPbI_2Br$/Spiro-MeOTAD/Ag	1.91	**1.06**	**0.85**	13.09	29
FTO/TiO_2/$CsPbI_2Br$/Spiro-OMeTAD/Au	1.92	**1.18**	**0.74**	13.54	30
FTO/Nb_2O_5/$CsPbI_2Br$/Carbon	1.90	**1.24**	**0.66**	12	31
ITO/SnO_2/$CsPbI_2Br$/Carbon	1.92	**1.27**	**0.65**	10.42	32
ITO/SnO_2/$CsPbI_2Br$/Spiro-MeOTAD/Ag	1.91	**1.23**	**0.68**	14.15	33
ITO/ETL/$CsPbI_2Br$/PDCBT/MoO_3/Ag	1.92	**1.30**	**0.62**	16.2	34
FTO/c-TiO_2/m-TiO_2/$CsPbI_2Br$/HTL/Au	1.92	**1.31**	**0.61**	14.86	35
ITO/NiO_x/$CsPbI_2Br$/c-Nb_2O_5/ETL/Bphen/Ag	2.00	**1.08**	**0.92**	11.17	36
FTO/TiO_2/$CsPbI_2Br$/Spiro-OMeTAD/Au	1.97	**1.10**	**0.87**	5.7	37
ITO/SnO_2/$CsPbI_2Br$/P3HT/Ag	1.91	**1.14**	**0.77**	12.22	38
ITO/SnO_2/$CsPbI_2Br$/PMMA/Carbon	1.91	**1.20**	**0.71**	10.95	39
FTO/NiMgLiO/CsPbI2Br/PCBM/BCP/Ag	1.92	**1.08**	**0.84**	11.05	40
ITO/TiO_2/$CsPbI_2Br$ NC/P3HT/Au	1.82	**1.32**	**0.50**	12.02	41
ITO/SnO_2/$CsPbI_2Br$/Spiro-MeOTAD/Au	**1.92**	**1.32**	**0.60**	**15.5**	**This work**

Table s2 Performance parameters of PCSs dependent on the concentration of CsI

CsI (y mg/mL)	V_{OC} (V)	E_{loss} (V)	J_{SC} (mA cm^{-2})	FF (%)	PCE (%) (Best)	PCE (%) (Average)
0	1.12	0.80	15.78	75.5	13.34	12.15
1	1.18	0.74	15.80	74.9	13.96	12.76
2	1.32	0.60	15.86	75.2	15.50	14.48
3	1.14	0.78	14.45	71.8	11.83	10.29
5	1.08	0.84	11.34	65.2	7.98	6.06

Table s3 Atom contents of perovskite thin films

Elements	***Control***			***Target-100nm***			***Target***		
	Wt%	*At%*	*At ratio*	*Wt%*	*At%*	*At ratio*	*Wt%*	*At%*	*At ratio*
Cs	18.89	19.72	1.00	20.01	20.45	1.00	19.71	20.55	1.00
Pb	31.07	20.28	1.03	30.85	20.22	0.99	29.99	20.06	0.98
I	38.59	40.12	2.03	38.44	41.14	2.01	43.36	47.35	2.30
Br	11.45	19.88	1.01	10.70	18.18	0.89	6.94	12.04	0.59

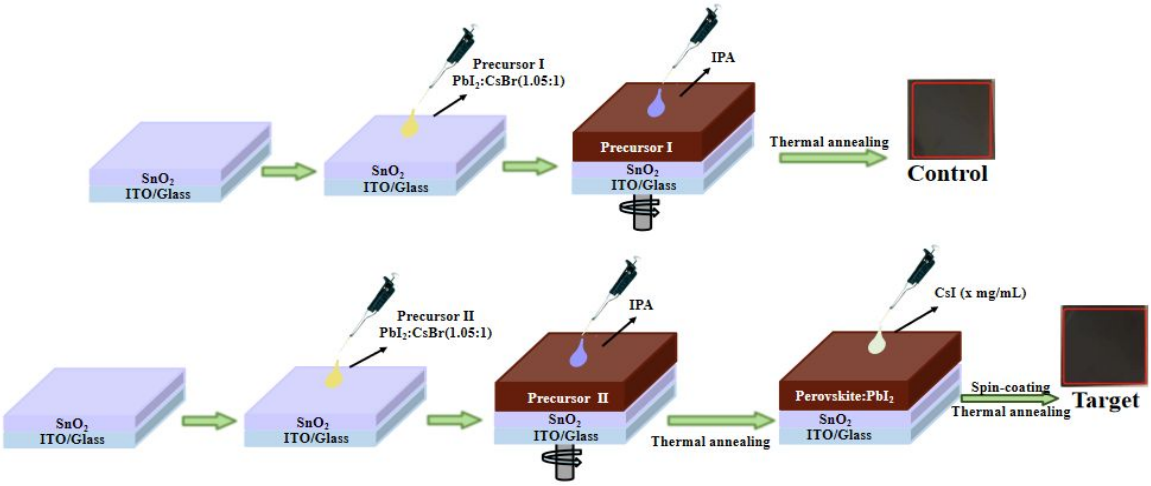

Fig. s1 The schematic illustration of $SnO_2/CsPbI_2Br$ and $SnO_2/CsPbI_2Br/(CsPbI_2Br)_{1-x}(CsPbI_3)_x$ thin films

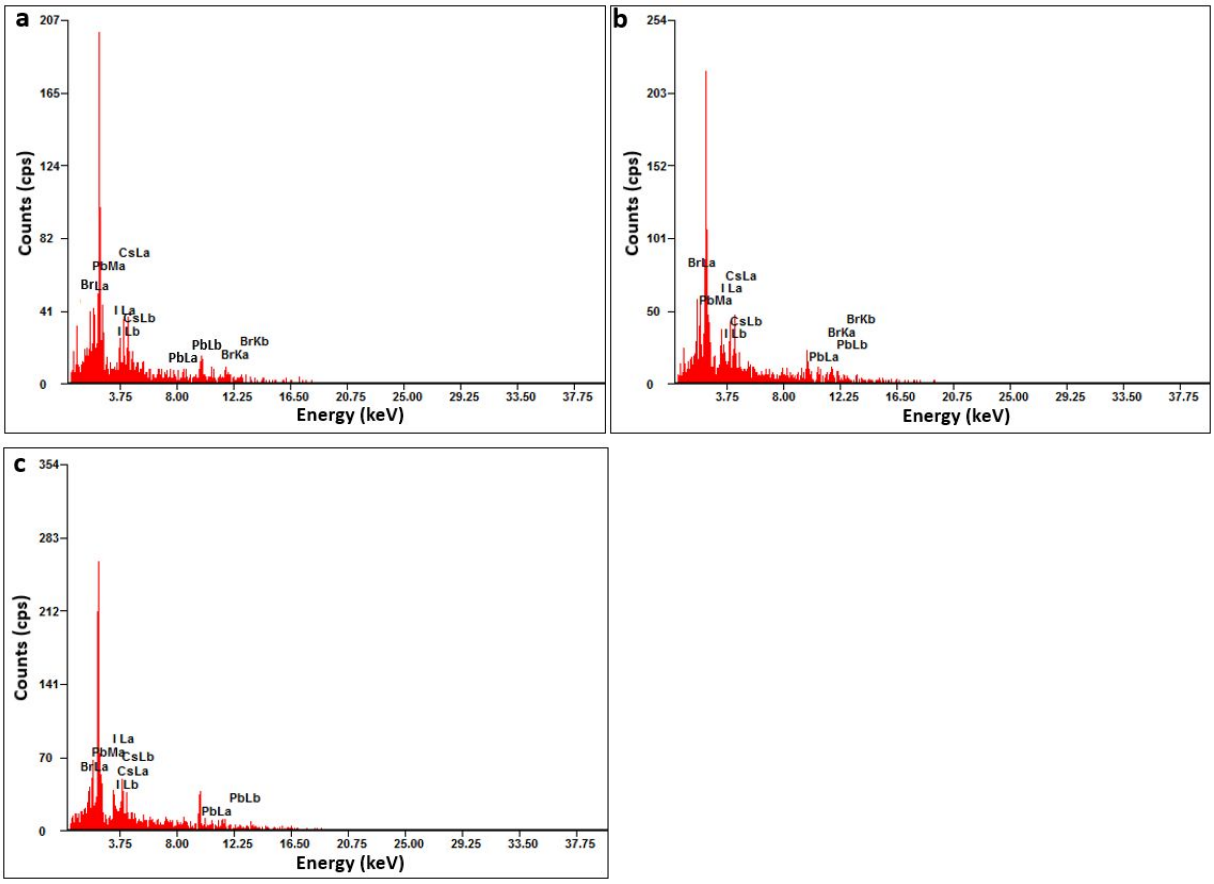

Fig. s2 EDX results of (a) control film, (b) target film with surface 100 nm scraped off and (c) target film.

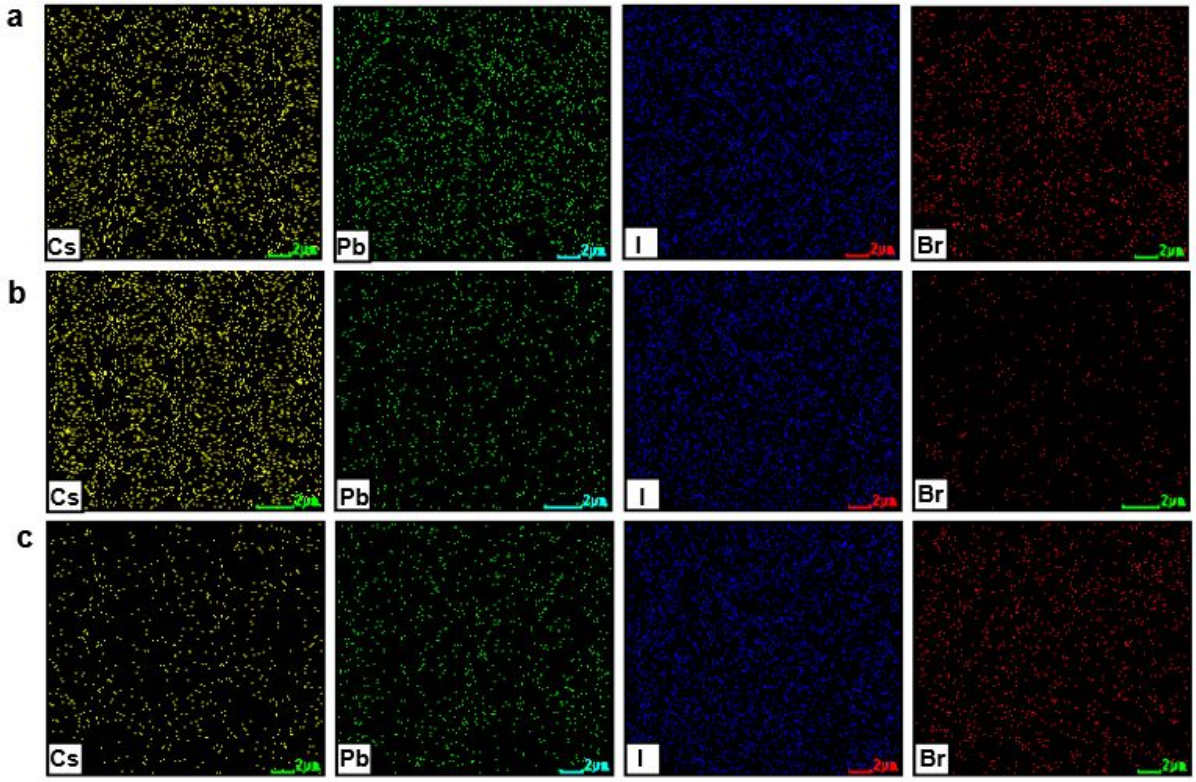

Fig. s3 EDX top view element mapping of (a) control film, (b) target film with surface 100 nm scraped off and (c) target film.

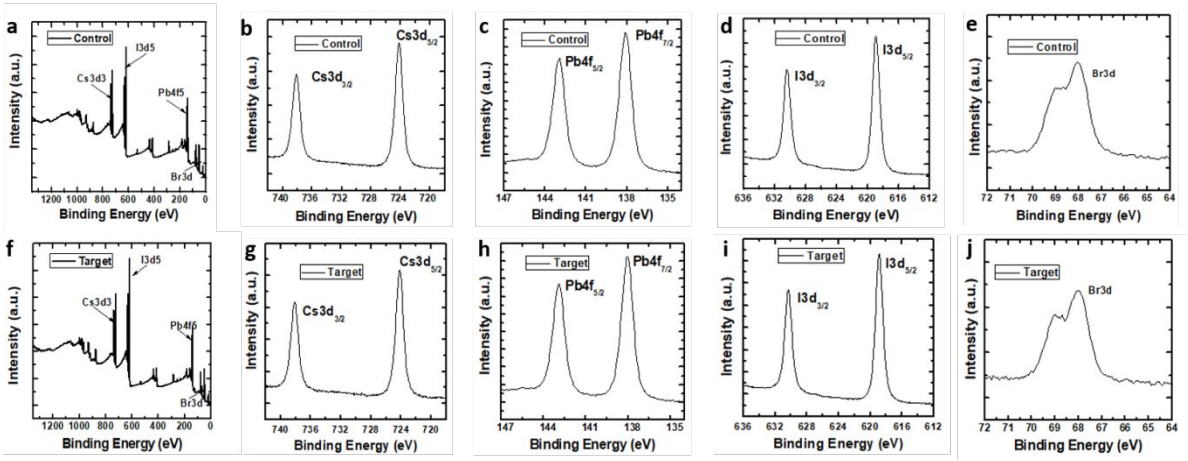

Fig. s4 XPS results of control (a) and target (f) thin film. corresponding (b, g) Cs 3d, (c, h) Pb 4f, (d, i) I 3d, and (e, j) Br 3d core-level spectra.

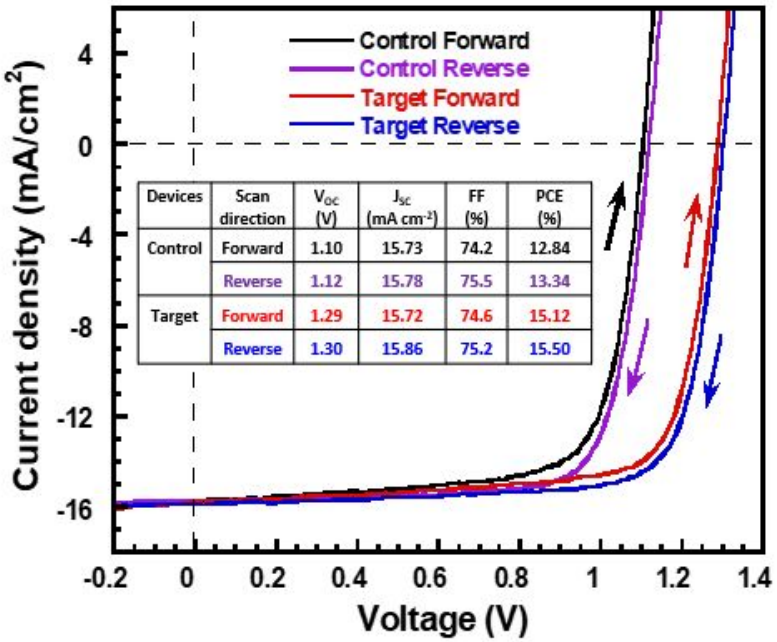

Devices	Scan direction	V_{OC} (V)	J_{SC} (mA cm^{-2})	FF (%)	PCE (%)
Control	Forward	1.10	15.73	74.2	12.84
	Reverse	1.12	15.78	75.5	13.34
Target	Forward	1.29	15.72	74.6	15.12
	Reverse	1.30	15.86	75.2	15.50

Fig. s5 The *J–V* characteristics of control and target PSCs measured from different scan direction.

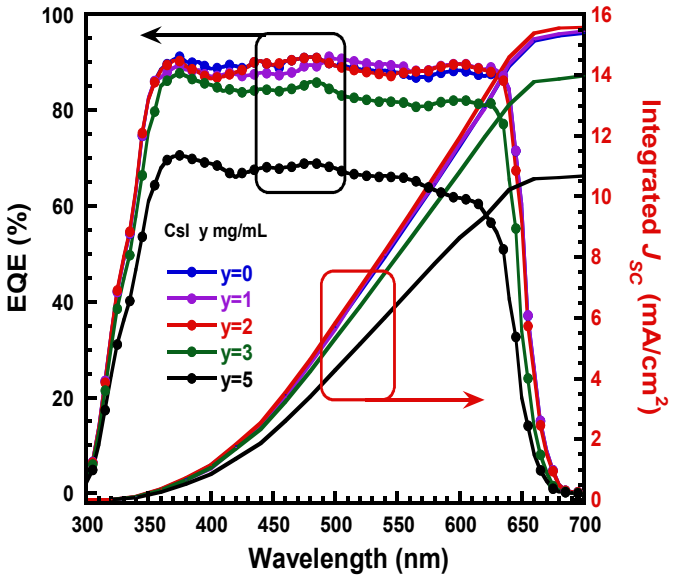

Fig. s6 The EQE spectrum and integrated J_{SC} of the PSCs with different concentration of CsI.

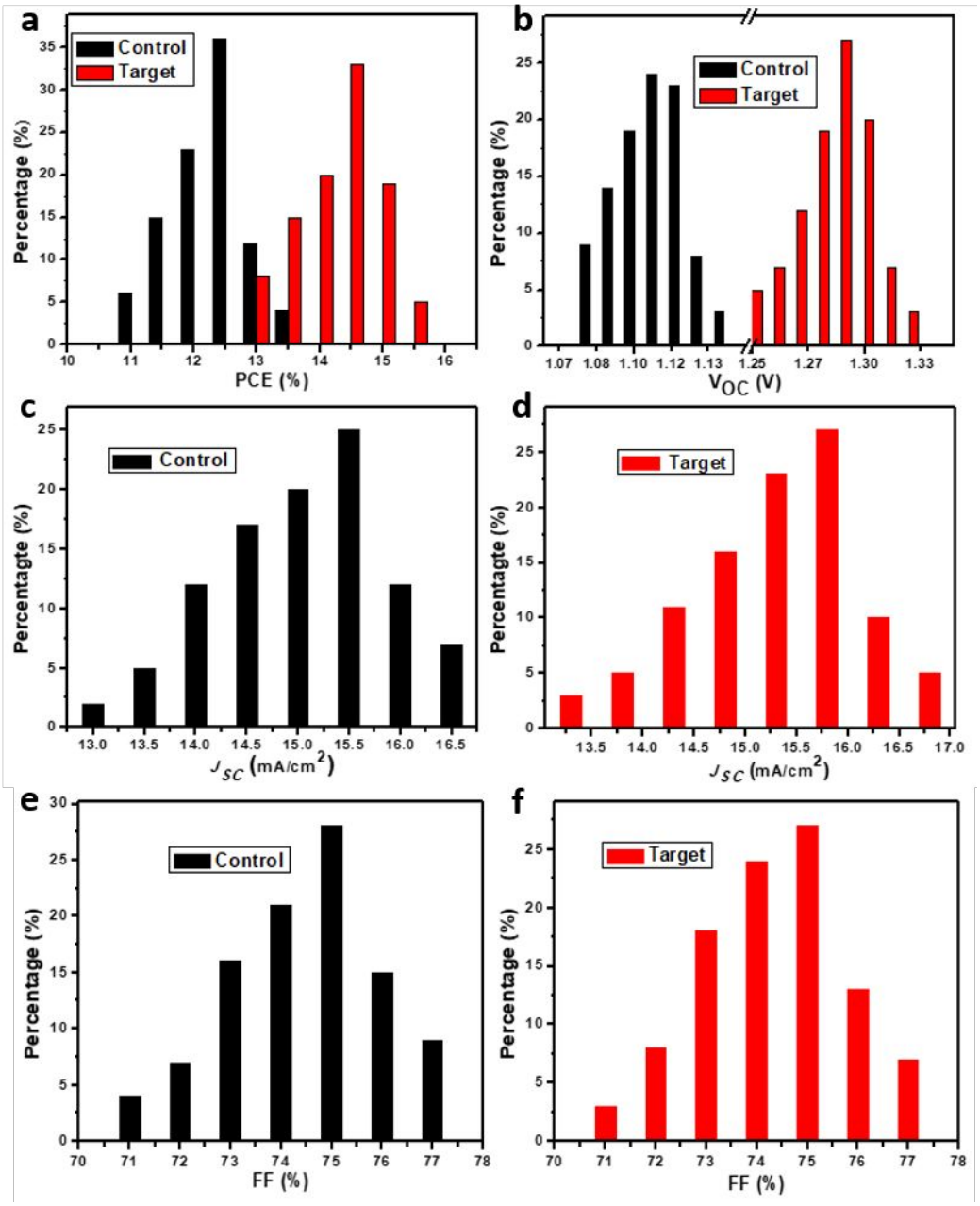

Fig. s7 The histograms of performance parameters of the control and target PSCs.

References

1. Beal, R. E.; Slotcavage, D. J.; Leijtens, T.; Bowring, A. R.; Belisle, R. A.; Nguyen, W. H.; Burkhard, G. F.; Hoke, E. T.; McGehee, M. D., Cesium Lead Halide Perovskites with Improved Stability for Tandem Solar Cells. *J. Phys. Chem. Lett.* **2016,** *7* (5), 746-51.

2. Sutton, R. J.; Eperon, G. E.; Miranda, L.; Parrott, E. S.; Kamino, B. A.; Patel, J. B.; Hörantner, M. T.; Johnston, M. B.; Haghighirad, A. A.; Moore, D. T., Bandgap-tunable Cesium Lead Halide Perovskites with High Thermal Stability for Efficient Solar Cells. *Adv. Energy Mater.* **2016,** *6* (8), 1502458.

3. Niezgoda, J. S.; Foley, B. J.; Chen, A. Z.; Choi, J. J., Improved Charge Collection in Highly Efficient $CsPbBrI_2$ Solar Cells with Light-induced Dealloying. *ACS Energy Lett.* **2017,** *2* (5), 1043-1049.

4. Nam, J. K.; Jung, M. S.; Chai, S. U.; Choi, Y. J.; Kim, D.; Park, J. H., Unveiling the Crystal Formation of Cesium Lead Mixed-Halide Perovskites for Efficient and Stable Solar Cells. *J. Phys. Chem. Lett.* **2017,** *8* (13), 2936-2940.

5. Zhou, W.; Zhao, Y.; Zhou, X.; Fu, R.; Li, Q.; Zhao, Y.; Liu, K.; Yu, D.; Zhao, Q., Light-Independent Ionic Transport in Inorganic Perovskite and Ultrastable Cs-based Perovskite Solar Cells. *J. Phys. Chem. Lett.* **2017,** *8* (17), 4122-4128.

6. Ma, Q.; Huang, S.; Chen, S.; Zhang, M.; Lau, C. F. J.; Lockrey, M. N.; Mulmudi, H. K.; Shan, Y.; Yao, J.; Zheng, J., The Effect of Stoichiometry on the Stability of Inorganic Cesium Lead Mixed-halide Perovskites Solar Cells. *J. Phys. Chem. C* **2017,** *121* (36), 19642-19649.

7. Wang, Y.; Zhang, T.; Xu, F.; Li, Y.; Zhao, Y., A Facile Low Temperature Fabrication of High Performance $CsPbI_2Br$ All-inorganic Perovskite Solar Cells. *Solar RRL* **2018,** *2* (1), 1700180.

8. Mariotti, S.; Hutter, O. S.; Phillips, L. J.; Yates, P. J.; Kundu, B.; Durose, K., Stability and Performance of $CsPbI_2Br$ thin Films and Solar Cell Devices. *ACS Appl. Mater. interfaces* **2018,** *10* (4), 3750-3760.

9. Liu, C.; Li, W.; Zhang, C.; Ma, Y.; Fan, J.; Mai, Y., All-Inorganic $CsPbI_2Br$ Perovskite Solar Cells with High Efficiency Exceeding 13%. *J. Am. Chem. Soc.* **2018,** *140* (11), 3825-3828.

10. Zhang, S.; Wu, S.; Chen, W.; Zhu, H.; Xiong, Z.; Yang, Z.; Chen, C.; Chen, R.; Han, L.; Chen, W., Solvent Engineering for Efficient Inverted Perovskite Solar Cells based on Inorganic $CsPbI_2Br$ Light Absorber. *Mater. today energy* **2018,** *8*, 125-133.

11. Jiang, Y.; Yuan, J.; Ni, Y.; Yang, J.; Wang, Y.; Jiu, T.; Yuan, M.; Chen, J., Reduced-dimensional α-$CsPbX_3$ Perovskites for Efficient and Stable Photovoltaics. *Joule* **2018,** *2* (7), 1356-1368.

12. Wang, P.; Zhang, X.; Zhou, Y.; Jiang, Q.; Ye, Q.; Chu, Z.; Li, X.; Yang, X.; Yin, Z.; You, J., Solvent-controlled Growth of Inorganic Perovskite Films in Dry Environment for Efficient and Stable Solar Cells. *Nat. Commun.* **2018,** *9* (1), 2225.

13. Yuan, J.; Zhang, L.; Bi, C.; Wang, M.; Tian, J., Surface Trap States Passivation for High-Performance Inorganic Perovskite Solar Cells. *Solar RRL* **2018,** *2* (10), 1800188.

14. Rao, H.; Ye, S.; Gu, F.; Zhao, Z.; Liu, Z.; Bian, Z.; Huang, C., Morphology Controlling of All-Inorganic Perovskite at Low Temperature for Efficient Rigid and Flexible Solar Cells. *Adv. Energy Mater.***2018,** *8* (23), 1800758.

15. Yan, L.; Xue, Q.; Liu, M.; Zhu, Z.; Tian, J.; Li, Z.; Chen, Z.; Chen, Z.; Yan, H.; Yip, H. L., Interface Engineering for All-Inorganic $CsPbI_2Br$ Perovskite Solar Cells with Efficiency over 14%. *Adv. Mater.* **2018,** *30* (33), 1802509.

16. Dong, C.; Han, X.; Zhao, Y.; Li, J.; Chang, L.; Zhao, W., A Green Anti-Solvent Process for High Performance Carbon-Based $CsPbI_2Br$ All-Inorganic Perovskite Solar Cell. *Solar RRL* **2018,** *2* (9), 1800139.

17. Zhang, L.; Li, B.; Yuan, J.; Wang, M.; Shen, T.; Huang, F.; Wen, W.; Cao, G.; Tian, J., High-voltage-efficiency Inorganic Perovskite Solar Cells in a Wide Solution-Processing Window. *J. Phys. Chem. Lett.* **2018,** *9* (13), 3646-3653.

18. Bian, H.; Bai, D.; Jin, Z.; Wang, K.; Liang, L.; Wang, H.; Zhang, J.; Wang, Q.; Liu, S. F., Graded Bandgap $CsPbI_{2+x}Br_{1-x}$ Perovskite Solar Cells with a Stabilized Efficiency of 14.4%. *Joule* **2018,** *2* (8), 1500-1510.

19. Bai, D.; Bian, H.; Jin, Z.; Wang, H.; Meng, L.; Wang, Q.; Liu, S. F., Temperature-assisted Crystallization for Inorganic $CsPbI_2Br$ Perovskite Solar Cells to Attain High Stabilized Efficiency 14.81%. *Nano energy* **2018,** *52*, 408-415.

20. Li, Y.; Wang, Y.; Zhang, T.; Yoriya, S.; Kumnorkaew, P.; Chen, S.; Guo, X.; Zhao, Y., Li Dopant Induces Moisture Sensitive Phase Degradation of An All-Inorganic $CsPbI_2Br$ Perovskite. *Chem. Commun.* **2018,** *54* (70), 9809-9812.

21. Chen, W.; Chen, H.; Xu, G.; Xue, R.; Wang, S.; Li, Y.; Li, Y., Precise Control of Crystal Growth for Highly Efficient $CsPbI_2Br$ Perovskite Solar Cells. *Joule* **2019,** *3* (1), 191-204.

22. Liu, C.; Li, W.; Li, H.; Wang, H.; Zhang, C.; Yang, Y.; Gao, X.; Xue, Q.; Yip, H.-L.; Fan, J.; Schropp, R. E. I.; Mai, Y., Structurally Reconstructed $CsPbI_2Br$ Perovskite for Highly Stable and Square-Centimeter All-Inorganic Perovskite Solar Cells. *Adv. Energy Mater.* **2019,** *9* (7), 1803572.

23. Yang, F.; Hirotani, D.; Kapil, G.; Kamarudin, M. A.; Ng, C. H.; Zhang, Y.; Shen, Q.; Hayase, S., All-Inorganic $CsPb_{1-x}Ge_xI_2Br$ Perovskite with Enhanced Phase Stability and Photovoltaic Performance. *Angew. Chem. Int. Ed. Engl.* **2018,** *57* (39), 12745-12749.

24. Lau, C. F. J.; Zhang, M.; Deng, X.; Zheng, J.; Bing, J.; Ma, Q.; Kim, J.; Hu, L.; Green, M. A.; Huang, S.; Ho-Baillie, A., Strontium-Doped Low-Temperature-Processed $CsPbI_2Br$ Perovskite Solar Cells. *ACS Energy Lett.* **2017,** *2* (10), 2319-2325.

25. Yin, G.; Zhao, H.; Jiang, H.; Yuan, S.; Niu, T.; Zhao, K.; Liu, Z.; Liu, S. F., Precursor Engineering for All-Inorganic $CsPbI_2Br$ Perovskite Solar Cells with 14.78% Efficiency. *Adv. Funct. Mater.* **2018,** *28* (39), 1803269.

26. Zeng, Z.; Zhang, J.; Gan, X.; Sun, H.; Shang, M.; Hou, D.; Lu, C.; Chen, R.; Zhu, Y.; Han, L., In Situ Grain Boundary Functionalization for Stable And Efficient Inorganic $CsPbI_2Br$ Perovskite Solar Cells. *Adv. Energy Mater.* **2018,** *8* (25), 1801050.

27. Zhang, J.; Bai, D.; Jin, Z.; Bian, H.; Wang, K.; Sun, J.; Wang, Q.; Liu, S. F., 3D-2D-0D Interface Profiling for Record Efficiency All-Inorganic $CsPbBrI_2$ Perovskite Solar Cells with Superior Stability. *Adv. Energy Mater.* **2018,** *8* (15), 1703246.

28. Nam, J. K.; Chai, S. U.; Cha, W.; Choi, Y. J.; Kim, W.; Jung, M. S.; Kwon, J.; Kim, D.; Park, J. H., Potassium Incorporation for Enhanced Performance and Stability of Fully Inorganic Cesium Lead Halide Perovskite Solar Cells. *Nano Lett* **2017,** *17* (3), 2028-2033.

29. Gao, Y.; Dong, Y.; Huang, K.; Zhang, C.; Liu, B.; Wang, S.; Shi, J.; Xie, H.; Huang, H.; Xiao, S.; He, J.; Gao, Y.; Hatton, R. A.; Yang, J., Highly Efficient, Solution-Processed $CsPbI_2Br$ Planar Heterojunction Perovskite Solar Cells via Flash Annealing. *ACS Photonics* **2018,** *5* (10), 4104-4110.

30. Jiang, H.; Feng, J.; Zhao, H.; Li, G.; Yin, G.; Han, Y.; Yan, F.; Liu, Z.; Liu, S. F., Low Temperature Fabrication for High Performance Flexible $CsPbI_2Br$ Perovskite Solar Cells. *Adv. Sci.* **2018,** *5* (11), 1801117.

31. Guo, Y.; Zhao, F.; Tao, J.; Jiang, J.; Zhang, J.; Yang, J.; Hu, Z.; Chu, J., Efficient and Hole-Transporting-Layer-Free $CsPbI_2Br$ Planar Heterojunction Perovskite Solar Cells through

Rubidium Passivation. *ChemSusChem* **2019,** *12* (5), 983-989.

32. Guo, Z.; Zhao, S.; Liu, A.; Kamata, Y.; Teo, S.; Yang, S.; Xu, Z.; Hayase, S.; Ma, T., Niobium Incorporation into $CsPbI_2Br$ for Stable and Efficient All-inorganic Perovskite Solar Cells. *ACS Appl. Mater. Interfaces* **2019,** 11(12), 19994-20003.

33. Khan, U.; Zhinong, Y.; Khan, A. A.; Zulfiqar, A.; Ullah, N., High-Performance $CsPbI_2Br$ Perovskite Solar Cells with Zinc and Manganese Doping. *Nanoscale Res. Lett.* **2019,** *14* (1), 116.

34. Tian, J.; Xue, Q.; Tang, X.; Chen, Y.; Li, N.; Hu, Z.; Shi, T.; Wang, X.; Huang, F.; Brabec, C. J.; Yip, H. L.; Cao, Y., Dual Interfacial Design for Efficient $CsPbI_2Br$ Perovskite Solar Cells with Improved Photostability *Adv. Mater.* 2019, e1901152.

35. Kim, D. H.; Heo, J. H.; Im, S. H., Hysteresis-Less $CsPbI_2Br$ Mesoscopic Perovskite Solar Cells with a High Open-Circuit Voltage Exceeding 1.3 V and 14.86% of Power Conversion Efficiency. *ACS Appl. Mater. Interfaces*, **2019,** 11(21), 19123-19131.

36. Han, D.; Xin, Y.; Yuan, Q.; Yang, Q.; Wang, Y.; Yang, Y.; Yi, S.; Zhou, D.; Feng, L.; Wang, Y., Solution-Processed 2D Nb_2O_5(001) Nanosheets for Inverted $CsPbI_2Br$ Perovskite Solar Cells: Interfacial and Diffusion Engineering. *Solar RRL* **2019**, 1900091.

37. Park, C.-G.; Choi, W.-G.; Na, S.; Moon, T., All-Inorganic Perovskite $CsPbI_2Br$ Through Co-evaporation for Planar Heterojunction Solar Cells. *Electronic Mater. Lett.* **2018,** *15*, 56-60.

38. Ye, Z.; Zhou, J.; Hou, J.; Deng, F.; Zheng, Y.-Z.; Tao, X., Low Temperature-Processed Stable and Efficient Carbon-Based $CsPbI_2Br$ Planar Perovskite Solar Cells by In Situ Passivating Grain Boundary and Trap Density. *Solar RRL* **2019**, 1900109.

39. Zhang, X.; Zhou, Y.; Li, Y.; Sun, J.; Lu, X.; Gao, X.; Gao, J.; Shui, L.; Wu, S.; Liu, J.-M., Efficient and Carbon-based Hole Transport Layer-free $CsPbI_2Br$ Planar Perovskite Solar Cells Using PMMA Modification. *J. Mater. Chem. C* **2019,** *7* (13), 3852-3861.

40. Zhang, S.; Wu, S.; Babu, B. H.; Chen, W.; Chen, R.; Huang, Y.; Yang, Z.; Zhu, H.; Zhou, J.; Chen, W., Adverse Oxidation of $CsPbI_2Br$ Perovskite during the Crystallization Process in an N_2 Glove-box. *J. Mater. Chem. C* **2019,** *7* (17), 5067-5073.

41. Zeng, Q.; Zhang, X.; Feng, X.; Lu, S.; Chen, Z.; Yong, X.; Redfern, S. A.; Wei, H.; Wang, H.; Shen, H., Polymer-Passivated Inorganic Cesium Lead Mixed-Halide Perovskites for Stable and Efficient Solar Cells with High Open-Circuit Voltage Over 1.3 V. *Adv. Mater.* **2018,** *30* (9), 1705393.